Journal of Materials Science manuscript

Regression Analysis of Temperature-Dependent Mechanical and Thermal Properties of Dielectric Technical Ceramics

Daithí de Faoite · David J. Browne · Kenneth T. Stanton

Received: date / Accepted: date

Abstract Regression analysis is performed on a dataset of temperature-dependent material properties of several ceramic materials. The materials considered are alumina, aluminium nitride, beryllia, fused quartz, sialon and silicon nitride. The properties considered are density, Young's, bulk and shear moduli, Poisson's ratio, tensile, flexural and compressive strength, thermal conductivity, specific heat capacity, and thermal expansion coefficient. The dataset, previously reported by the current authors [1], was compiled to facilitate the materials selection and design of a ceramic component for the Variable Specific-Impulse Magnetoplasma Rocket (VASIMR®). Temperature-dependent material property data are required for accurate thermo-structural modelling of such ceramic components which operate over a wide temperature range. The goal of this paper is to calculate a set of regression coefficients to reduce this dataset to a tractable format for use in the materials selection and design of such components. Regression analysis could not be performed for all material properties for all of these materials, due to a lack of data in the literature, and these gaps in the available data are highlighted.

Keywords regression analysis · ceramics · thermal properties · mechanical properties

1 Introduction

Representative material property data, given as a function of temperature where possible, have been gathered from the literature, reviewed, and previously reported by the current

D. de Faoite
School of Mechanical and Materials Engineering, University College Dublin, Belfield, Dublin 4, Ireland

D. J. Browne
School of Mechanical and Materials Engineering, University College Dublin, Belfield, Dublin 4, Ireland

K. T. Stanton*
School of Mechanical and Materials Engineering, University College Dublin, Belfield, Dublin 4, Ireland
*Corresponding Author:
Tel.: +353-1-716-1918
Fax: +353-1-283-0534
E-mail: Kenneth.Stanton@ucd.ie

authors for material specifications of alumina, aluminium nitride, beryllia, fused quartz, sialon and silicon nitride [1]. The material specifications have been chosen to best reflect advanced commercially available material grades. The compiled dataset is not a review of all existing data, but a representative summary of data for commercially-available material grades. Property data in the open literature is sparse for some material properties for certain materials; in particular for fused quartz and sialon materials, and for tensile and compressive strength properties.

These material property data have been collated to aid in the materials selection and design of a gas containment tube (GCT) for the helicon section of the Variable Specific-Impulse Magnetoplasma Rocket (VASIMR®) [2–5], an advanced electric propulsion rocket currently being developed by the Ad Astra Rocket Company, Houston, Texas. This dataset can be used in the engineering design of ceramic component with complementary material requirements, such as the selection of materials for microwave and RF waveguide windows, dielectric components in ion engines and hall thrusters, dielectric heat spreaders in electronics, as well as components for other advanced plasma devices such as ITER [6, 7].

For ceramic components which may experience high temperatures during operation, consideration of the variation of material properties with temperature is essential for accurate modelling and materials selection. Regression analysis is performed on the temperature dependence of material property data from this dataset for alumina, aluminium nitride, beryllia, fused quartz, sialon and silicon nitride. The goal of the regression analysis is to calculate a set of regression coefficients which, in conjunction with the regression functions, form a simplified, self-consistent representation of the material property dataset. Reducing the dataset to regression data allows design engineers to efficiently use the data. Such data are particularly useful for use in numerical simulations; e.g. such as [7–9]. The resulting regression data can be used by design engineers in the initial stages of design, to model the performance of systems containing these materials over a wide range of temperatures.

The material properties which are independent of each other are analysed independently. The related material properties of Young's, bulk, and shear moduli and Poisson's ratio are analysed simultaneously in order to yield a self-consistent dataset. The procedure used to analyse related material properties simultaneously is described in Section 2.3. Regression analysis was not possible for every material property for each material, due to the limited data available,but have been presented where possible. The material properties considered here are listed in Table 1. Representative room temperature values, are given in Table 2 for ease of reference.

Table 1 Material properties considered.

Mechanical	Thermal
Density	Thermal Conductivity
Young's Modulus	Specific Heat Capacity
Bulk Modulus	Thermal Expansion Coefficient
Shear Modulus	
Poisson's Ratio	
Tensile Strength	
Flexural Strength	
Compressive Strength	

It is recognised that some observed quantities, such as density, elastic moduli, Poisson's ratio, specific heat capacity and thermal expansion coefficient, are directly related to inter-

Table 2 Representative room temperature (20 °C) material property values. Values given in this table may differ somewhat from values calculated from the curve fit equations. Due to the nature of the fitting procedure the curve fit line does not always pass directly through the value for the best estimate of the room temperature property value.

Property	Units	Alumina	Aluminium Nitride	Beryllia	Fused Quartz	Sialon	Silicon Nitride
Density	$g{\cdot}cm^{-3}$	3.91	3.28	2.85	2.20	3.32	3.21
Young's Modulus	GPa	400	320	–	72.5	–	–
Shear Modulus	GPa	160	130	–	31.0	–	–
Bulk Modulus	GPa	255	195	–	37.0	–	–
Poisson's Ratio	-	0.24	0.23	–	0.17	–	–
Flexural Strength	MPa	380	320	225	–	–	775
Tensile Strength	MPa	265	–	–	–	–	660
Compressive Strength	GPa	3.0	–	–	–	–	–
Specific Heat Capacity	$J{\cdot}kg^{-1}{\cdot}K^{-1}$	765	715	990	730	725	680
Thermal Conductivity	$W{\cdot}m^{-1}{\cdot}K^{-1}$	32.0	170	270	1.35	11.5	31.5
Instantaneous CTE	$\times 10^{-6}\ K^{-1}$	5.28	2.29	5.50	0.43	1.34	1.35
Average CTE	$\times 10^{-6}\ K^{-1}$	5.13	2.16	5.40	0.41	1.23	1.27

atomic bonding. These may be referred to as 'intrinsic material properties'. Other observed quantities, such as flexural, tensile and compressive strength, and thermal conductivity are strongly dependent upon external factors such as processing, forming, finishing, environmental conditions, and the details of the testing procedure. These may be referred to as 'extrinsic material quantities', due to their dependence on external factors. However in this paper both intrinsic material properties and extrinsic observed quantities are referred to as 'material properties' for simplicity.

2 Regression Procedure

All curve fitting in this work is done on a least-squares basis. Regression models are used which represent a mathematical relationshp between the independent variable and the observations. A residual ε_i is defined as the difference between the observed data value y_i and the predicted data value $\hat{y}_i$ from the regression model f:

$$\varepsilon_i = y_i - \hat{y}_i \tag{1}$$

The sum-of-squares method seeks to find the coefficients of the regression model by minimising SS, the sum of the square of the residuals:

$$\mathrm{SS}(a,b\ldots) = \sum_{i=1}^{N} \varepsilon_i^2 = \sum_{i=1}^{N} (y_i - \hat{y}_i)^2 \tag{2}$$

$$= \sum_{i=1}^{N} \big(y_i - f(x_i,a,b\ldots)\big)^2 \tag{3}$$

where $a,b\ldots$ are the curve fit coefficients used in this particular curve fit model; the number used depends on the model. y_i is an observation value, observed at independent variable value x_i, and f is the curve fit model. This form of the sum of squares is termed the unweighted sum of squares.

Non-linear regression models are used in this study, requiring the use of an iterative solver. The trust-region algorithm implemented in MATLAB® (The MathWorks®, 3 Apple Hill Drive, Natick, MA 01760-2098, USA; MATLAB® Version 7.4.0.0287 (R2007a)) is used in this study for this purpose.

No claim is made of the regression models representing the underlying physics of the variation of the material properties with temperature; they simply act as convenient mathematical expressions. For each material property, the simplest curve fitting model available that adequately describes the data is used. A summary of the regression functions used is given in Table 3, and their individual use will be justified in Sections 2.2.2 to 2.2.5 and in Section 2.3 of the current paper.

Table 3 Summary of regression functions used. The units of temperature used for all regression fits are degrees Celsius (°C).

Property	Materials	Function	Equation
Young's Modulus	Alumina, Aluminium Nitride	$E(T) = aT^2 + bT + c$	22
	Fused Quartz	$E(T) = aT^3 + bT^2 + cT + d$	19
Shear Modulus	Alumina, Aluminium Nitride	$G(T) = aT^2 + bT + c$	22
	Fused Quartz	$G(T) = aT^3 + bT^2 + cT + d$	19
Bulk Modulus	Alumina, Aluminium	$K(T) = aT^2 + bT + c$	22
	Fused Quartz	$K(T) = aT^3 + bT^2 + cT + d$	19
Flexural Strength	Alumina	$\sigma(T) = a - \frac{b}{1 + c\exp(-dT)}$	9
	Aluminium Nitride, Silicon Nitride	$\sigma_f(T) = a - bT^2$	11
	Beryllia	$\sigma_f(T) = a - b(T - c)^2$	12
Tensile Strength	Alumina	$\sigma_t = a - b\left(\frac{1}{\sqrt{1 + c\exp(-dT)}}\right)$	10
	Silicon Nitride	$\sigma_t(T) = a - bT^2$	11
Compressive Strength	Alumina	$\sigma_c(T) = aT^2 + bT + c$	22
Specific Heat Capacity	Alumina, Aluminium Nitride, Beryllia, Sialon, Silicon Nitride	$c_P(T) = a + bT - c\exp(-dT)$	13
	Fused Quartz	$c_P(T) = aT^4 + bT^3 + cT^2 + dT + e$	15
Thermal Conductivity	Alumina	$\lambda(T) = a + \frac{b\exp(-cT)}{T + d}$	16
	Aluminium Nitride, Beryllia	$\lambda(T) = \frac{a\exp(-bT)}{T + c}$	17
	Fused Quartz	$\lambda(T) = aT^4 + bT^3cT^2 + dT + e$	15
	Sialon, Silicon Nitride	$\lambda(T) = a + \frac{b}{T + c}$	18
Instantaneous CTE	Alumina, Aluminium Nitride, Beryllia, Sialon, Silicon Nitride	$\alpha(T) = a + bT - c\exp(-dT)$	13
	Fused Quartz	$\alpha(T) = aT^3 + bT^2 + cT + d$	19
Average CTE	Alumina, Aluminium Nitride, Beryllia, Sialon, Silicon Nitride	$\bar{\alpha}(T) = a + bT - c\exp(-dT)$	13
	Fused Quartz	$\bar{\alpha}(T) = aT^3 + bT^2 + cT + d$	19

2.1 Weightings

The dataset analysed contains experimental observations from numerous different experiments [1], and differing numbers of observations are reported from each experiment. A procedure is required to ensure that experiments reporting observations at closely spaced temperature intervals do not unduly influence the calculation of the regression coefficients

over those experiments reporting observations at fewer temperatures. This is done by calculating weightings for each observation.

For each material property, data is obtained from J different experiments. Some experiments report many data points as a function of temperature, while others report a single data point at a single temperature. The assumption is made that each experiment, whether yielding one or many data points, is of equal validity, and thus should be given equal weighting in the curve fitting process. If each individual data point were given equal weighting, experiments reporting data at closely spaced temperature intervals would predominate over those reporting data more sparsely with temperature.

The number of observations in each of the J experiments is denoted K^j, $1 \leq j \leq J$, where K^j will in general be different for each experiment. The total number of observations from all experiments is denoted N. The weight assigned to each observation w_k^j is given by:

$$w_k^j = \frac{N}{J \times K^j} \tag{4}$$

For the weighting w_k^j, the superscript j indicates that the weighting pertains to data from experiment j, $1 \leq j \leq J$, while the subscript k indicates that the weighting is for the observation k from that experiment, $1 \leq k \leq K$. The total weighting given to the experiment j—that is, the sum of the individual weightings for all observations in the experiment—is:

$$w^j = \sum_{k=1}^{K^j} w_k^j = K^j \times \left(\frac{N}{J \times K^j} \right) = \frac{N}{J} \tag{5}$$

Therefore, the experiment has the same total weighting of N/J, independent of the number of observations in each experiment. The sum of all weightings w_{tot} is given by:

$$w_{\text{tot}} = \sum_{j=1}^{J} w^j = J \times \left(\frac{N}{J} \right) = N \tag{6}$$

The un-weighted sum-of-squares is equivalent to having a weighting of 1 for all observations, in which case the sum of all weightings would also be N.

Thus, we will use weighted least-squares regression, minimising the following sum of squares:

$$\text{SS}\,(a,b\ldots) = \sum_{i=1}^{N} w_i \,(y_i - \hat{y}_i)^2 \tag{7}$$

$$= \sum_{i=1}^{N} w_i \big(y_i - f\,(x_i,a,b\ldots)\big)^2 \tag{8}$$

Here w_i are the weightings of each observation, $1 \leq i \leq N$.

2.2 Independent Curve Fitting

Density, flexural, tensile and compressive strength, specific heat capacity, thermal conductivity and coefficient of thermal expansion are considered independently in this work. The details relating to the regression analysis of these material properties are discussed in this section.

2.2.1 Density

Density measurements come from both X-ray diffraction measurements and direct density estimates [1]. These two measurements are used together for some but not all materials to estimate density.

Density variations with temperature are related to thermal expansion coefficients. However, in general the change in density with temperature is very small, and in any case for numerical simulations, changes in density may be calculated automatically by numerical software from thermal expansion coefficients.

For density, the variation with temperature is not considered, and the average of room temperature density data is taken for each material. Thus, a curve fitting procedure is not required.

2.2.2 Flexural, Tensile and Compressive Strength

Munro [10] uses the following regression model for the flexural strength of alumina:

$$y(T) = a - \frac{b}{1 + c\exp(-dT)} \tag{9}$$

and uses the following one for the tensile stregth of alumina:

$$y(T) = a - b\left(\frac{1}{\sqrt{1 + c\exp(-dT)}}\right) \tag{10}$$

where T is temperature (°C). For the compressive strength of alumina, Munro uses a quadratic polynomial. For the flexural, tensile and compressive strength of alumina, only a small number of additional sources could be found over those identified in the Munro review. Therefore, the regression functions and coefficients recommended by Munro for these properties are used here also, and are given in Table 3 and Table 4, respectively.

For the flexural strength of aluminium nitride, and the flexural and tensile strength of silicon nitride, the following regression function is used:

$$y(T) = a - bT^2 \tag{11}$$

For beryllia there are large difference between the data of Beaver et al. [11], Carniglia et al. [12] and Fryxell & Chandler [13]. This leads to there being no satisfactory way to fit one function to all the data. Due to the fact that the experimental method of Fryxell & Chandler is described very clearly, and the fact that the data of Fryxell & Chandler is intermediate to that of Beaver et al. and Carniglia et al., the data of Fryxell & Chandler alone is used for the current regression analysis of beryllia. Unlike alumina, aluminium nitride or silicon nitride, it is clear from the data that there is an increase in flexural strength in beryllia at intermediate temperatures. Thus, the regression functions used for alumina, aluminium nitride or silicon nitride are not suitable. Instead, the following quadratic function is used:

$$y(T) = a + b(T - c)^2 \tag{12}$$

For fused quartz no temperature-dependent data exist in the original dataset. For sialon only one RT flexural strength value and one value at elevated temperatures is given. Therefore, no regression analysis is performed for flexural or tensile strength for these materials.

The absence of intermediate temperature data for ceramics leads to uncertainty in the form the regression model should take. In this work regression functions which yield the lowest sum of error estimate (SEE) are chosen.

2.2.3 Specific Heat Capacity

The regression function used by Munro [10] for alumina is:

$$y(T) = a + bT - c\exp(-dT) \tag{13}$$

For fused quartz a polynomial is used. In order to choose the polynomial degree to use for fused quartz, polynomials of increasing degree were fit to the data. The fit order at which the variance σ^2, as computed below, showed no further statistically significant decrease, provides the best model [14]:

$$\sigma^2 = \frac{\sum_{i=1}^{N} \varepsilon_i^2}{N-m-1} \tag{14}$$

where σ^2 is the variance, ε are the residuals, N is the number of data points and m is the degree of the polynomial. For this dataset, the variance was a minimum for a fourth degree polynomial:

$$y(T) = aT^4 + bT^3 + cT^2 + dT + e \tag{15}$$

2.2.4 Thermal Conductivity

For alumina the following regression function, used by Munro [10], is used:

$$y(T) = a + \frac{b\exp(-cT)}{T+d} \tag{16}$$

For aluminium nitride and beryllia a modified form of Equation (16), without the constant term, is used here:

$$y(T) = \frac{a\exp(-bT)}{T+c} \tag{17}$$

This provides a fit with a lower SEE than the un-modified equation, yielding a better fit for these materials than Equation (16).

For fused quartz, curve fits are presented for both the true and effective thermal conductivity. All data up to 350 °C is used in the regression analysis of both true and effective thermal conductivity. For the effective thermal conductivity, above 350 °C data of Sugawara [15] is used. For the true thermal conductivity, above 350 °C data of Sergeev et al. [16] is used. Fourth-degree polynomials, Equation 15 are used for both properties. For fitting sialon, the following function was found to provide a fit with a lower SEE than either Equation 16 or Equation 17, and was thus used:

$$y(T) = a + \frac{b}{T+c} \tag{18}$$

This is in essence a simplified version of the Munro equation without the exponential term.

2.2.5 Coefficient of Thermal Expansion

In this work regression analysis is performed independently on coefficient of thermal expansion (CTE) data. For crystalline materials, the macroscopic CTE and the lattice parameters are inter-related properties. Where lattice parameter data are also available, global regression analysis can be performed on these and macoscopic CTE data in order to yield the best overall data set.

Data for mean and instantaneous CTE, definitions of which may be found in [1], must be clearly distinguished. In this work 0 °C is taken as the reference temperature for the mean CTE. Curve fitting is first performed for instantaneous CTE data. A corresponding curve fit for the mean CTE is then calculated from this using the relevant equation.

One form of fitting function that can be used for CTE is Equation 13, the functional form used by Munro [10] for CTE, (the same as the functional form used by Munro for specific heat capacity). This functional form can be used either for the mean or instantaneous CTE. For alumina, Equation 13 is used in this work. The data of Munro [10] is for the mean CTE, so this has been converted to instantaneous CTE values. For aluminium nitride and for beryllia the data presented by Slack & Bartram [17], not included in the preceeding work by the current authors [1], are considered the most reliable are used as the recommended curve. The regression coefficients in Table 4 for aluminium nitride and beryllia are for a curve fit of these data.

For fused quartz, a cubic polynomial is used as the regression model:

$$y(T) = aT^3 + bT^2 + cT + d \tag{19}$$

For sialon, only the thermal expansion data of Swab et al. [19] is available. It is deemed that there is insufficient data to perform a curve fit.

2.3 Global Curve Fitting of Elastic Properties

For isotropic materials the Young's modulus (E), bulk modulus (K), shear modulus (G) and Poisson's ratio (ν) are inter-related by simple relations. Although the crystals of ceramics considered here are anisotropic, the macroscopic polycrystalline material may be considered pseudo-isotropic. In this work, curve fits are created simultaneously for these material properties. The advantage of this approach is that it ensures self-consistent curve fits, as the inter-relations are built into the fitting procedure. An additional advantage is to provide a better curve fit for each property, by leveraging experimental data from all properties.

Although some variation in Poisson's ratio does occur with temperature, this variation is typically small. Thus, here the Poisson's ratio is assumed to be constant with respect to temperature. This assumption greatly simplifies the temperature-dependent inter-relations between the elastic properties. The assumption makes the variations in E, K and G with respect to temperature linearly proportional to each other. The same form of fitting equation is used for these three properties. Each curve fit has three coefficients: z_0, z_1, z_2 for Young's modulus; k_0, k_1, k_2 for bulk modulus; and g_0, g_1, g_2 for shear modulus. These coefficients are not independent and are related by the proportionality between E, K and G. However, the numerical value of the proportionality is not known *a priori*, and is determined implicitly in the least squares minimisation. We have four independent variables to optimise: z_0, z_1, z_2 and ν. We minimise an objective function—a sum of squared error terms. The problem is re-configured as a constrained optimisation problem, subject to the constraints imposed by the elastic moduli equations. An equation is constructed for each data point of each

material property to characterise its deviation from the curve fit equation for that material property. The deviation measures for all data points from the four material properties are then simultanesouly minimised in the least-squares sense.

As was done for the independent regression analysis discussed in Sections 2.1–2.2, the assumption is made that each experiment is of equal validity, and is thus assigned equal weighting. Here, the weightings used are w_ν, w_E, w_G and w_K, for Poisson's ratio, Young's, shear and bulk moduli, respectively. These account for the differing numbers of data points reported from each experiment, ensuring that experiments for which a large number of data-points are reported, are not given disproportionate influence. Additionally, these weightings used for the global regression analysis of the elastic properties account for the different numerical magnitudes of ν, E, G and K. The weighting used for each data-point is:

$$w_k^j = \left(\frac{N}{J \times K^j}\right)\left(\frac{1}{y_k^j}\right)^2 \tag{20}$$

Here y_k^j is the observation k, $1 \leq k \leq K$ from experiment j, $1 \leq j \leq J$, while w_k^j is the weighting relating to that observation. The residuals which are minimised thus characterise the deviation from each data-point as a fraction of the value of the data-point.

The Wachtman equation [20] has been shown to work well to describe the temperature dependence of Young's modulus or bulk modulus over a wide range of temperatures:

$$Y(T) = Y_0 - B \cdot T \cdot \exp\left(\frac{-T_0}{T}\right) \tag{21}$$

wherere Y_0 is the Young's or bulk modulus at 0 K, and both T_0 [K] and B [GPa.K^{-1}] are empirical fitting parameters, related to the Debye temperature and Grüneisen parameter. The parameter T_0 is relatively sensitive to small variations or errors in Young's or bulk moduli data [21].

For the polycrystalline ceramics, the simultaneous curve fitting procedure was initially attempted using the Wachtman equation. However, it was found that the parameter T_0 was too sensitive to scatter in the data. Therefore, a simple quadratic polynomial regression model is used here instead:

$$y = aT^2 + bT + c \tag{22}$$

In contrast to polycrystalline ceramics, the elastic moduli of fused quartz increase with increasing temperature. For fused quartz a simple cubic polynomial (Equation 19) is used, as per the approach previously discussed in Section 2.2.3:

In order to define the error functional, expressions are written for the deviation from the curve fit equation:

$$\varepsilon_{\nu,i} = \nu_i - \nu \tag{23}$$

$$\varepsilon_{E,i} = E_i - \left(z_0 T_i^2 + z_i T_i + z_2\right) \tag{24}$$

$$\varepsilon_{G,i} = G_i - \left[\left(z_0 T_i^2 + z_1 T_i + z_2\right)\left(\frac{1}{2+2\nu}\right)\right] \tag{25}$$

$$\varepsilon_{K,i} = K_i - \left[\left(z_0 T_i^2 + z_1 T_i + z_2\right)\left(\frac{1}{3-6\nu}\right)\right] \tag{26}$$

Here ν_i, E_i, G_i and K_i are the value of the regression function for Poisson's ratio, Young's modulus, shear and bulk moduli, respectively, at the value of independent variable corresponding to data point i, $1 \leq i \leq N$. The objective function for minimisation is:

$$\mathrm{SS}(z_0, z_1, z_2, \nu) = \sum_{i=1}^{N_\nu} w_i (\varepsilon_{\nu,i})^2 + \sum_{i=1}^{N_E} w_i (\varepsilon_{E,i})^2 + \sum_{i=1}^{N_G} w_i (\varepsilon_{G,i})^2 + \sum_{i=1}^{N_K} w_i (\varepsilon_{K,i})^2 \tag{27}$$

Here N_ν, N_E, N_G and N_K are the number of data-points for Poisson's ratio, Young's, shear and bulk moduli respectively.

One limitation of the global curve-fitting method is that it does not work well for sparse datasets. In this work, global curve fitting of the elastic properties has been performed for alumina, aluminium nitride and fused quartz. However, for beryllia, sialon and silicon nitride there were insufficient data in the available dataset to successfully perform global curve fitting. Another limitation of the global curve-fitting method, particularly when used in conjunction with a weighting system, is that outlier data values can have a significant effect on the calculated curve fit. For the elastic properties of alumina and aluminium nitride, outlier values were omitted from the global regression analysis. This resulted in the calculation of a better fit for the remaining data.

3 Results

Curve fit coefficients are given in Table 4, along with cross-references to the applicable equation from the preceeding analysis. Representative material property values at 20 °C are given in Table 2. Representative property values at 20 °C may differ slightly from the value calculated from the curve fit equation at 20 °C.

Values of Poisson's ratio calculated from global curve fitting of the elastic properties are as follows: alumina $\nu = 0.2401$, aluminium nitride $\nu = 0.2250$, fused quartz $\nu = 0.1723$. These values are used as the representative values of Poisson's ratio at 20 °C, and are given in Table 2, rounded to two significant figures.

Data values and calculated regression fits for five material properties for fused quartz are plotted in Figure 1. Data values and calculated regression fits for thermal conductivity of the six materials considered in this study are plotted in Figure 2.

All coefficients determined here are given to four significant figures in order to ensure accurate reconstruction of the curve fit.

4 Conclusions

Regression analysis has been performed, where possible, on several material properties for the six materials of interest. Insufficient data were available to allow for reliable curve fitting of all material properties for all materials. A paucity of data exists for tensile strength, bulk modulus, and in particular compressive strength of these materials. Clearly, experimental work is required to address this lack of material property data in the peer-reviewed open literature.

References

1. de Faoite, D., Browne, D.J., Chang-Díaz, F.R., Stanton, K.T.: A review of the processing, composition, and temperature-dependent mechanical and thermal properties of dielectric technical ceramics. Journal of Materials Science **47**(10), 4211–4235 (2012)

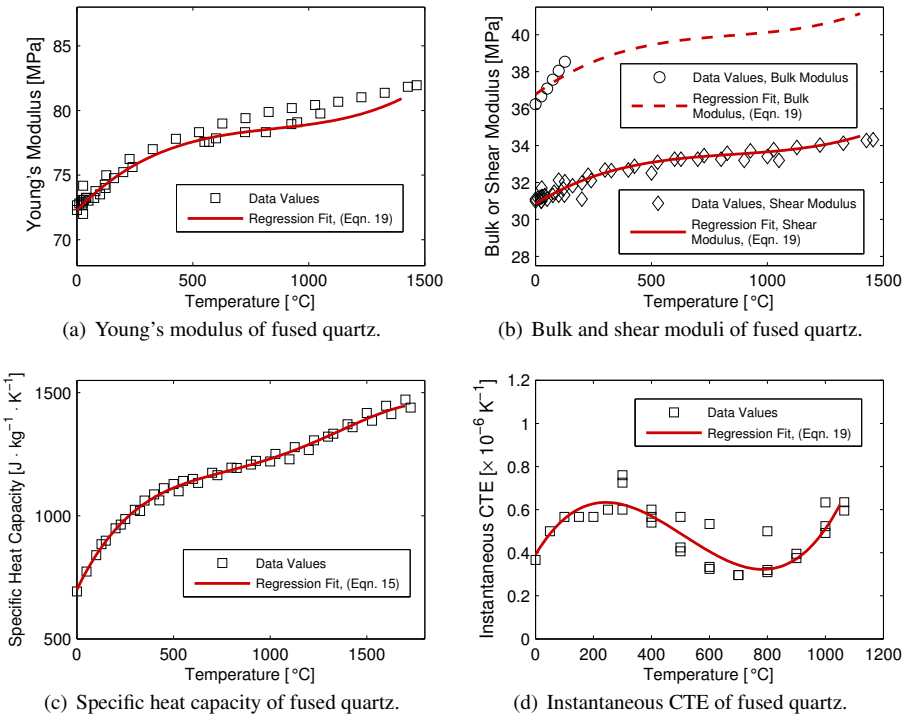

(a) Young's modulus of fused quartz.

(b) Bulk and shear moduli of fused quartz.

(c) Specific heat capacity of fused quartz.

(d) Instantaneous CTE of fused quartz.

Fig. 1 Data values and calculated regression fits for five material properties for fused quartz: (a) Young's modulus, (b) bulk and shear moduli, (c) specific heat capacity, (d) instantaneous CTE.

2. Chang-Díaz, F.R., Squire, J.P., Ilin, A.V., McCaskill, G.E., Nguyen, T.X., Winter, D.S., Petro, A.J., Goebel, G.W., Cassady, L.D., Stokke, K.A., Dexter, C.E., Graves, T.P., Amador Jr., L., George, J.A., Carter, M.D., Baity Jr., F.W., Barber, G.C., Goulding, R.H., Sparks, D.O., Schwenterly, S.W., Bengston, R.D., Breizman, B.N., Jacobson, V.T., Arefiev, A.V., Sagdeev, R.Z., Karavasilis, K., Novakovski, S.V., Chan, A.A., Glover, T.W.: The development of the VASIMR engine. International Conference on Electromagnetics in Advanced Applications, Torino, Italy, 1999
3. Chang-Diaz, F.R.: The VASIMR rocket. Scientific American **283**(5), 90–97 (2000)
4. Chang-Díaz, F. R., Squire, J. P., Bengston, R. D., Breizman, B. N., Baity, F. W., Carter, M. D.: The physics and engineering of the VASIMR engine. 36th AIAA/ASME/SAE/ASEE Joint Propulsion Conference, Huntsville, Alabama, July 17–19, 2000
5. Mulcahy, J. M., Browne, D. J., Stanton, K. T., Chang Diaz, F. R., Cassady, L. D., Berisford, D. F., Bengston, R. D.: Heat flux estimation of a plasma rocket helicon source by solution of the inverse heat conduction problem. International Jouarnal of Heat and Mass Transfer **52**(9–10), 2343–2357 (2009)
6. Heikkinen, J. A., Orivuori, S., Linden, J., Saarelma, S., Heikinheimo, L.: Thermal and electrical analysis of alumina and beryllia coax high-power windows under irradiation. IEEE Transactions on Dielectrics and Electrical Insulation **6**(2), 169–174 (1999)
7. Hamlyn-Harris, C., Borthwick, A., Fanthome, J., Waldon, C., Nightingale, M., Richardson, N.: Engineering design of an RF vacuum window for the ITER ICRH antenna. Fusion Engineering and Design **84** 887–894 (2009)
8. Huang, X., Garner, J., Conroy, P.: Thermal analysis for a 37-mm gun chamber with ceramic nozzles. Technical Report ARL-MR-624, Army Research Laboratory, 2005
9. Cazajus, V., Lorrain, B., Welemane, H., Parantheon, Y., Karama, M.: Thermo-mechanical behaviour of ceramic metal brazed assemblies. Proc. IMechE Part L: J. Mterials: Design and Applications **222**, 291–297 (2008)
10. Munro, R.: Evaluated material properties for a sintered alpha-alumina. Journal of the American Ceramic Society **80**(8), 1919–1928 (1997)

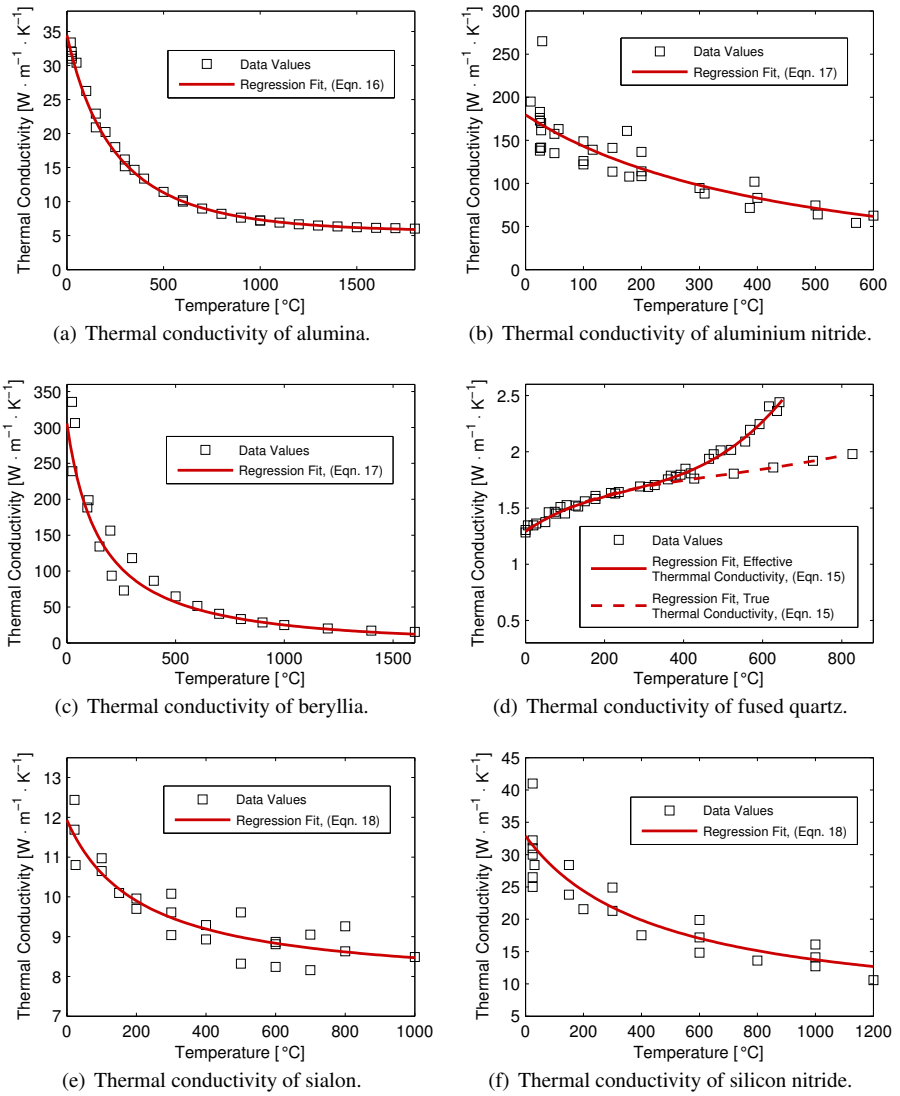

(a) Thermal conductivity of alumina.

(b) Thermal conductivity of aluminium nitride.

(c) Thermal conductivity of beryllia.

(d) Thermal conductivity of fused quartz.

(e) Thermal conductivity of sialon.

(f) Thermal conductivity of silicon nitride.

Fig. 2 Data values and calculated regression fits for thermal conductivity of the six materials considered in this study: (a) alumina, (b) aluminium nitride, (c) beryllia, (d) fused quartz, (e) sialon, (f) silicon nitride.

11. Beaver, W. W., Theodore, J. G., Bielawski, C. A.: Effects of powder characteristics, additives and atmosphere on the sintering of sulfate-derived BeO. Journal of Nuclear Materials **14**, 326–337 (1964)
12. Carniglia, S. C., Johnson, R. E., Hott, A. C., Bentle G. G.: Hot pressing for nuclear applications of BeO; process, product, and properties Journal of Nuclear Materials **14**, 378–394 (1964)
13. Fryxell, R. E., Chandler, B. A.: Creep, strength, expansion, and elastic moduli of sintered BeO as a function of grain size, porosity, and grain orientation Journal of the American Ceramic Society **47**(6), 283-291 (1964)
14. Gerald, C.F., Wheatley, P.O.: Applied Numerical Analysis, 7th edn. Pearson Education, Inc., Boston (2004)

15. Sugawara, A.: Precise determination of thermal conductivity of high purity fused quartz from 0° to 650°C. Physica **41**(3), 515–520 (1969)
16. Sergeev, O.A., Shashkov, A.G., Umanskii, A.S.: Thermophysical properties of quartz glass. Journal of Engineering Physics and Thermophysics **43**, 1375–1383 (1982)
17. Slack, G.A., Bartram, S.F.: Thermal expansion of some diamondlike crystals. Journal of Applied Physics **46**(1), 89–98 (1975)
18. Lillie, J.: Some properties of beryllium oxide. Tech. Rep. UCRL-6457, Lawrence Radiation Laboratory, University of California, Livermore, California (1961)
19. Swab, J.J., Wereszczak, A.A., Tice, J., Caspe, R., Kraft, R. H., Adams, J.W.: Mechanical and thermal properties of advanced ceramics for gun barrel applications. Technical Report ARL-TR-3417, Army Research Laboratory, 2005
20. Wachtman, J., Tefft, W., Lam, D., Apstein, C.: Exponential temperature dependence of Young's modulus of several oxides. Physical Review **122**(6), 1754–1759 (1961)
21. Bruls, R.J., Hintzen, H.T., de With, G., Metselaar, R.: The temperature dependence of the Young's modulus of $MgSiN_2$, AlN and Si_3N_4. Journal of the European Ceramic Society **21**(3), 263–268 (2001)

Table 4 Regression coefficients for material properties. An entry of '–' for all coefficients indicates that no recommended curve fit can be given, due to insufficient data for this material. *Effective thermal conductivity for fused quartz; includes effects of heat transfer enhancement due to radiation. †Regression coefficients recommended by Munro [10]. The temperature range over which the curve-fit is valid is given. Units for individual coefficients are not stated, but may be derived from the regression function, if required. The units of temperature used for all regression fits are degrees Celsius (°C).

Property Unit	Material	Fit Equation	a	b	c	d	e	Valid Range [°C]
Young's Modulus GPa	Alumina	22	-18.50×10^{-6}	-13.78×10^{-3}	398.5			0–1400
	Aluminium Nitride	22	-10.46×10^{-6}	-19.92×10^{-3}	319.0			0–1700
	Beryllia	–	–	–	–	–	–	–
	Fused Quartz	19	7.455×10^{-9}	-19.04×10^{-6}	18.19×10^{-3}	72.31		0–1400
	Sialon	–	–	–	–	–	–	–
	Silicon Nitride	–	–	–	–	–	–	–
Shear Modulus GPa	Alumina	22	-7.459×10^{-6}	-5.557×10^{-3}	160.7			0–1400
	Aluminium Nitride	22	-4.269×10^{-6}	-8.131×10^{-3}	130.2			0–1700
	Beryllia	–	–	–	–	–	–	–
	Fused Quartz	19	3.180×10^{-9}	-8.122×10^{-6}	7.759×10^{-3}	30.84		0–1400
	Sialon	–	–	–	–	–	–	–
	Silicon Nitride	–	–	–	–	–	–	–
Bulk Modulus GPa	Alumina	22	-11.86×10^{-6}	-8.839×10^{-3}	255.5			0–1400
	Aluminium Nitride	22	-6.340×10^{-6}	-12.07×10^{-3}	193.4			0–1700
	Beryllia	–	–	–	–	–	–	–
	Fused Quartz	19	3.791×10^{-9}	-9.683×10^{-6}	9.250×10^{-3}	36.77		0–1400
	Sialon	–	–	–	–	–	–	–
	Silicon Nitride	–	–	–	–	–	–	–
Flexural Strength MPa	Alumina†	9	380.5	137×10^{3}	176×10^{3}	3.9×10^{-3}		20–1500
	Aluminium Nitride	11	322.0	99.19×10^{-6}				0–1400
	Beryllia	12	244.0	117.9×10^{-6}	436.9			0–1200
	Fused Quartz	–	–	–	–	–	–	–
	Sialon	–	–	–	–	–	–	–
	Silicon Nitride	11	777.6	215.6×10^{-6}				0–1300
Tensile Strength MPa	Alumina†	10	267	256	5.8×10^{9}	18×10^{-3}		20–1500
	Aluminium Nitride	–	–	–	–	–	–	–
	Beryllia	–	–	–	–	–	–	–
	Fused Quartz	–	–	–	–	–	–	–
	Sialon	–	–	–	–	–	–	–
	Silicon Nitride	11	661.9	251.7×10^{-6}				0–1400
Compressive Strength GPa	Alumina	22	1.1×10^{-6}	-3.5×10^{-3}	3.1			20–1400
	Aluminium Nitride	–	–	–	–	–	–	–
	Beryllia	–	–	–	–	–	–	–
	Fused Quartz	–	–	–	–	–	–	–
	Sialon	–	–	–	–	–	–	–
	Silicon Nitride	–	–	–	–	–	–	–
Specific Heat Capacity $J{\cdot}kg^{-1}{\cdot}K^{-1}$	Alumina	13	1.159×10^{3}	111.1×10^{-3}	436.1	5.271×10^{-3}		0–1800
	Aluminium Nitride	13	1.093×10^{3}	222.5×10^{-3}	429.8	5.859×10^{-3}		0–1400
	Beryllia	13	1.915×10^{3}	173.5×10^{-3}	996.0	3.800×10^{-3}		0–1800
	Fused Quartz	15	-3.523×10^{-10}	1.509×10^{-6}	-2.236×10^{-3}	1.610	700.5	0–1700
	Sialon	13	1.152×10^{3}	94.48×10^{-3}	465.4	4.177×10^{-3}		0–1000
	Silicon Nitride	13	1.237×10^{3}	14.69×10^{-3}	592.4	3.140×10^{-3}		0–1400
Thermal Conductivity $W{\cdot}m^{-1}{\cdot}K^{-1}$	Alumina	16	5.527	9.829×10^{3}	1.406×10^{-3}	339.8		0–1800
	Aluminium Nitride	17	92.29×10^{3}	490.5×10^{-6}	513.9			0–600
	Beryllia	17	48.35×10^{3}	515.8×10^{-6}	158.2			0–1600
	Fused Quartz	15	-2.122×10^{-12}	5.433×10^{-9}	-4.872×10^{-6}	2.344×10^{-3}	1.294	0–800
	Fused Quartz*	15	-1.702×10^{-12}	9.503×10^{-9}	-6.502×10^{-6}	2.479×10^{-3}	1.291	0–650
	Sialon	18	7.732	896.6	213.6			0–1000
	Silicon Nitride	18	4.983	12.78×10^{3}	458.0			0–1200
Instantaneous CTE $\times10^{-6}$ K^{-1}	Alumina	13	8.264	1.354×10^{-3}	3.323	4.965×10^{-3}		0–1600
	Aluminium Nitride	13	8.112	-1.240×10^{-3}	6.092	2.486×10^{-3}		0–1000
	Beryllia	13	51.39	-9.918×10^{-3}	46.09	432.8×10^{-6}		0–1500
	Fused Quartz	19	3.917×10^{-9}	-6.030×10^{-6}	2.233×10^{-3}	390.8×10^{-3}		0–1050
	Sialon	13	2.000	2.199×10^{-3}	900.1×10^{-3}	12.56×10^{-3}		0–1000
	Silicon Nitride	13	3.669	387.1×10^{-6}	2.484	3.172×10^{-3}		0–1300
Mean CTE $\times10^{-6}$ K^{-1}	Alumina	13	7.481	918.1×10^{-6}	2.519	3.010×10^{-3}		0–1600
	Aluminium Nitride	13	6.028	-86.47×10^{-6}	4.008	1.750×10^{-3}		0–1000
	Beryllia	13	33.47	-3.983×10^{-3}	28.18	319.3×10^{-6}		0–1500
	Fused Quartz	19	979.2×10^{-12}	-2.010×10^{-6}	1.117×10^{-3}	390.8×10^{-3}		0–1050
	Sialon	13	1.819	1.215×10^{-3}	707.7×10^{-3}	7.122×10^{-3}		0–1000
	Silicon Nitride	13	2.905	407.6×10^{-6}	1.719	2.144×10^{-3}		0–1300